

The Conformation of the Poly(ethylene glycol) Chain in Mono-PEGylated Lysozyme and Mono-PEGylated Human Growth Hormone

Sheetal S. Pai,[†] Boualem Hammouda,[§] Kunlun Hong,^{||} Danilo C. Pozzo,[⊥] Todd M. Przybycien,^{*,†,‡} and Robert D. Tilton^{*,†,‡}

[†]Center for Complex Fluids Engineering, Department of Chemical Engineering, and [‡]Department of Biomedical Engineering, Carnegie Mellon University, Pittsburgh, Pennsylvania 15213, United States

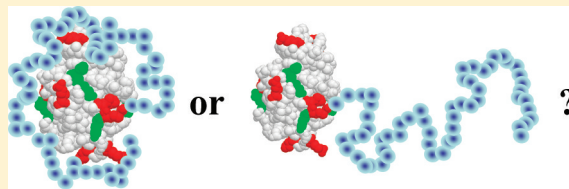
[§]NIST Center for Neutron Research, National Institute of Standards and Technology, Gaithersburg, Maryland 20899, United States

^{||}Center for Nanophase Materials Sciences and Chemical Science Division, Oak Ridge National Laboratory, Oak Ridge, Tennessee 37831, United States

[⊥]Department of Chemical Engineering, University of Washington, Seattle, Washington 98195, United States

S Supporting Information

ABSTRACT: Covalent conjugation of poly(ethylene glycol) or “PEGylation” has proven an effective strategy to improve pharmaceutical protein efficacy by hindering recognition by proteases, inhibitors, and antibodies and by retarding renal clearance. Because it determines the strength and range of intermolecular steric forces and the hydrodynamic properties of the conjugates, the configuration of protein-conjugated PEG chains is the key factor determining how PEGylation alters protein in vivo circulation time. Mono-PEGylated proteins are typically described as having a protective PEG shroud wrapped around the protein, but recent dynamic light scattering studies suggested that conjugates adopt a dumbbell configuration, with a relatively unperturbed PEG random coil adjacent to the globular protein. We used small-angle neutron scattering (SANS) to distinguish between the dumbbell model and the shroud model for chicken-egg lysozyme and human growth hormone covalently conjugated to a single 20 kDa PEG chain. The SANS contrast variation technique was used to isolate the PEG portion of the conjugate. Scattering intensity profiles were well described by the dumbbell model and inconsistent with the shroud model.



INTRODUCTION

Covalent conjugation of poly(ethylene glycol) (PEG) to proteins, PEGylation, has proven to be an effective strategy to increase in vivo circulation times of protein therapeutics, with consequent improvements in pharmaceutical efficacy.¹ The benefits derive from decreased renal clearance rates, decreased proteolytic degradation, and decreased immune response.^{1–4} Decreased renal clearance is attributed to the larger hydrodynamic radius of the conjugates that hinders glomerular filtration. Protective effects are attributed to steric and hydration repulsions between PEGylated proteins and other activity-degrading proteins,⁵ including immunoproteins, proteases, or inhibitors. These protective effects can accrue without loss of protein biological activity, depending on the number, molecular weight, and location of the attached PEG chains on the protein. PEGylation may also enhance protein thermal stability, making some conjugates more resistant to unfolding than their unmodified counterparts.⁶ Examples of PEGylated proteins that have been approved for therapeutic use by the U.S. Food and Drug Administration include PEGasys (interferon α -2a; Genentech USA, Inc.), PEG-Intron (interferon α -2b; Merck & Co., Inc.), Neulasta (granulocyte colony-stimulating factor;

Amgen), Adagen (adenosine deaminase; Sigma-Tau Pharmaceuticals, Inc.), Oncaspar (L-asparaginase; Sigma-Tau Pharmaceuticals, Inc.), and Somavert (growth hormone; Pfizer).⁷ Recent work in this laboratory and others^{8–11} indicates that PEG conjugation may also significantly improve the preservation of protein native structure and bioactivity during sustained release from biodegradable depots, in part by modifying the damaging interactions between the conjugates and the interfaces that they encounter during encapsulation and release.

Understanding the configuration of PEG chains when conjugated to proteins is necessary to interpret the steric protective effect and hindered renal clearance for circulating proteins in vivo and conjugate adsorption and associated denaturation in sustained-release delivery devices. Additionally, this information is important for interpreting filtration behavior¹² and chromatographic behavior^{13,14} of PEGylated proteins during purification operations.

The commonly presumed structure of mono-PEGylated proteins is the shroud model, according to which an attached

Received: July 7, 2011

Revised: September 22, 2011

Published: September 28, 2011

PEG chain wraps around the protein to create a shielding effect.^{5,7,13–21} Lacking direct probes of the grafted PEG conjugate structure, investigators have relied on the shroud model to interpret hydrodynamic or thermodynamic measurements. For example, Fee and Van Alstine analyzed the size exclusion chromatographic behavior of PEG-conjugated proteins in terms of the protein shroud model.¹³ Using three proteins (α -lactalbumin, β -lactoglobulin dimer, and bovine serum albumin), each conjugated with one or more PEG chains having one of three different molecular masses (2.4, 5.6, or 22.5 kDa), the authors concluded that the protein and conjugated PEG interacted to create a spheroid complex in which the PEG formed a layer surrounding the protein; this morphological model and corresponding geometrically based predictions did represent size exclusion chromatography retention times well for both mono-PEGylated and poly-PEGylated conjugates.¹³ García-Arellano et al. used the shroud model to interpret data on the thermal stability of horse heart cytochrome *c* singly or multiply modified with 0.35, 0.75, or 2 kDa PEG;¹⁵ the authors presumed that the PEG acts as a cage and coils around the protein surface.¹⁵ Manjula et al. used molecular dynamics simulations to predict the configuration of 5, 10, and 20 kDa PEG chains attached to hemoglobin; they concluded that instead of passively extending from the surface of the protein, the PEG chain folds upon itself in a separate domain on the surface of the protein.¹⁴ While the shroud model may be appropriate for multiple PEG chains attached to a protein, we investigate the conformation of one PEG chain attached to a protein as motivated by the current pharmaceutical relevance of mono-PEGylated species. Early development of PEGylated protein therapeutics was based on grafting several low molecular weight PEG chains (5 kDa); however, the trend is toward grafting a smaller number of larger PEG chains, such as 20 kDa linear PEG or 40 kDa branched PEG grafts that provide improved performance relative to the multiply conjugated proteins.^{5,19} The current work is motivated by a competing model for the configuration of protein-conjugated PEG chains in mono-PEGylated species: the dumbbell model wherein the PEG conjugate exists as a relatively unperturbed random coil adjacent to, but not surrounding, the protein.

The configuration of a random coil polymer chain in solution is dictated by polymer segment excluded volume interactions and the configurational entropy of the chain. We contend that the entropic cost of wrapping a PEG chain around a globular protein that has a radius of gyration that is comparable to that of the PEG would be prohibitive. It should be noted that absent a large externally applied pressure, PEG chains do not adsorb to proteins, so there is little or no enthalpic driving force to wrap the PEG around the protein. Using dynamic light scattering (DLS), we determined that the hydrodynamic diameter of a monoPEG–lysozyme conjugate was comparable to the sum of the individual diameters of a single lysozyme plus a single 20 kDa PEG. The diffusion coefficient determined by DLS could be interpreted in terms of a cylinder having a length equal to the sum of the unperturbed PEG and lysozyme hydrodynamic diameters.⁹ The same trend was observed previously in our group for ribonuclease A (RNase A) and monoPEG–RNase A.⁸ Because the protein and polymer have similar dimensions in solution, it is unlikely that a single 20 kDa PEG chain would be able to wrap around these proteins. The DLS data for the monoPEG–protein conjugates support a dumbbell model. Similarly, in a study of partition coefficients obtained from size exclusion chromatography data for PEG, proteins, and the corresponding PEGylated proteins, Molek and Zydney

determined that the effective spherical volume of PEGylated proteins could be estimated as the sum of the volumes of the protein and free PEG. The sieving coefficients were consistent with the conjugated PEG chains behaving as a random coil.¹² Fee later showed that these estimates hold true for systems where the PEG chain is substantially larger than the protein itself.²² He et al. compared small-angle X-ray scattering (SAXS) and small-angle neutron scattering (SANS) data in order to draw conclusions about the shape of di-PEGylated human galectin; their findings support the dumbbell model.²³ The authors found a slight compression of the random coils with increased solution concentration of the PEGylated protein.²³ Finally, Svergun et al. used SAXS to study PEG-conjugated hemoglobin and reported that the major part of the PEG chain protrudes away from hemoglobin.²⁴ The authors also stated that a portion of the PEG chain interacts with the protein.²⁴

The distinction between the shroud and the dumbbell models remains unresolved, because the effective conjugate sizes that would be predicted by the two models fall within the margin of error for the conventional macromolecular sizing techniques available. Thus, purely size-based methods, which are inherently indirect methods of characterizing polymer configuration, are incapable of adequately discriminating between the two prevailing conjugate models.

We used SANS as a direct method to discriminate between the dumbbell and the shroud models. This approach takes particular advantage of the unique ability to contrast match the aqueous medium with individual portions of the conjugate to exclusively probe the conformation of the remainder of the conjugate. This is not possible with X-ray or light scattering in aqueous systems. Here, we report the configuration of a single 20 kDa PEG chain grafted to either 14 kDa chicken-egg lysozyme or 22 kDa human growth hormone (HGH), grafted predominantly at the N terminus. Using mixtures of D₂O and H₂O to isolate the scattering from the PEG portion of the conjugate, we conclude that a single conjugated PEG chain exists as a random coil with dimensions similar to those of the free PEG chains in solution. The contrast-matched SANS data were well described by the random coil form factor, confirming the suitability of the dumbbell model for these conjugates. This conclusion was further supported by the inability to fit SANS data to a core–shell form factor model that would capture a polymer shell wrapped around a protein core, without resorting to unphysical model parameters. Because of its relevance to protein therapeutics, we also investigated the configuration of the PEG conjugate in a plasmalike, high oncotic pressure environment, finding similar configurations for the PEG conjugates in dilute solution and in the model plasmalike environment.

■ EXPERIMENTAL PROCEDURES

Materials. Chicken-egg lysozyme (Sigma-Aldrich Co., catalog no. L-6876) and deuterium oxide (Cambridge Isotopes, D > 99%) were used without further purification. HGH was donated by Genentech Inc. Methoxy-PEG–propionaldehyde (mPEG–PA), 20.7 kDa, was donated by Dr. Reddy's Laboratories (Cambridge, United Kingdom) and used without further purification. A sample of 22.2 kDa perdeuterated mPEG–PA (*dm*PEG–PA) was synthesized by the Center for Structural Molecular Biology (CSMB) Bio-Deuteration Laboratory at Oak Ridge National Laboratory and used without further purification. The molecular weights of the hydrogenated and deuterated mPEG–PA samples were determined by matrix-assisted laser desorption/ionization (MALDI) mass

spectrometry (PerSeptive Voyager STR MS, Applied Biosystems). The average degrees of polymerization for the hydrogenated mPEG-PA and the deuterated mPEG-PA were 470 and 461, respectively. Conjugation reaction and conjugate purification buffers were prepared from sodium phosphate monobasic and dibasic anhydrous salts (Fisher Scientific, 99% pure) and sodium chloride (Sigma-Aldrich Co., 99% pure). Sodium cyanoborohydride (Sigma-Aldrich Co., 95% pure) and 4-(2-hydroxyethyl)-1-piperazineethanesulfonic acid (HEPES, Sigma-Aldrich Co., $\geq 95\%$ pure) were used as received. All water was purified by reverse osmosis followed by treatment to 18 M Ω /cm resistivity using a Barnstead NANOpure Diamond system. Synthesis of dmPEG-PA is described in the Supporting Information, S1.

Protein PEGylation and Conjugate Characterization.

We reacted lysozyme with either the ~ 20 kDa hydrogenated mPEG-PA (*hm*PEG-PA) or the deuterated mPEG-PA (*dm*PEG-PA) (1:6 mol ratio) in a pH 5.1, 100 mM sodium phosphate buffer containing 20 mM sodium cyanoborohydride, conditions established to strongly favor N-terminal PEGylation of the protein,²⁵ and fractionated the product into monoPEGylated and diPEGylated samples by size exclusion chromatography as described in detail previously.⁹ We used MALDI mass spectrometry to determine the number of PEG molecules attached to lysozyme in each collected fraction, as described previously.⁹ The location of the PEG modification was determined previously to be primarily the N-terminal lysine, with slight modification at lysine residues 33 and 97.⁹ To obtain an appropriate concentration, we pooled together the purified monoPEG-lysozyme fractions from eight separate PEGylations, for both the *hm*PEG-PA and the *dm*PEG-PA. The pooled monoPEG-lysozyme samples then underwent several rounds of buffer exchange into 10 mM HEPES, pH 7.4, using a diafiltration technique with 3000 MWCO centrifugal filter units (Millipore, catalog no. UFC900324). HGH was reacted with *dm*PEG-PA (1:6 mol ratio), separated, and buffer exchanged in the same manner described above for lysozyme.

The secondary structures of the lysozyme conjugates were characterized to determine if PEGylation resulted in structural perturbations using circular dichroism (CD) spectroscopy (J-810 Spectropolarimeter, Jasco, Inc.). Far UV CD spectra of unmodified lysozyme and hydrogenated monoPEG-lysozyme and deuterated monoPEG-lysozyme indicate that the secondary structure of lysozyme was not significantly altered upon PEGylation (Figure S1 in the Supporting Information, S2). The CD spectra were further analyzed using CD Pro software²⁶ to provide quantitative estimates of secondary structure contents (Table S1 in the Supporting Information, S2). Results indicate that conjugate secondary structure estimates were consistent with those of the unmodified protein. Finally, all samples, in pH 7.4 10 mM HEPES buffer, were dried on a lyophilizer (Unitrap II, VirTis) before transporting them with ice packs to be reconstituted for SANS experiments. Lyophilization did not significantly impact the secondary structure of the lysozyme conjugates, as determined by CD (data not shown).

SANS. SANS experiments were performed at the National Institute of Standards and Technology (NIST) Center for Neutron Research (NCNR) using the 30 m SANS instrument NG3²⁷ and at Oak Ridge National Laboratory (ORNL) using the 30 m Bio-SANS instrument at the High Flux Isotope Reactor (HFIR). Each lyophilized sample was suspended in the appropriate medium (H₂O, D₂O, or H₂O-D₂O mixture) at room temperature and immediately loaded into quartz cells

with a 1 mm path length. At NIST, a neutron wavelength of 6 Å was used at three detector distances (1.3, 4, and 13 m) to gather scattering profiles. At ORNL, two detector distances, 0.3 and 6 m, were used to gather scattering profiles. The SANS data were fully reduced by referencing an open beam neutron flux and subtracting the background incoherent scattering. All scattering profiles were analyzed using IGOR Pro macros developed at NIST.²⁸

The H₂O-D₂O composition points of minimum scattering intensity for lysozyme and HGH were first determined using contrast variation on pure lysozyme and pure HGH samples in solutions containing various hydrogen isotope ratios (D/H). The ratio at which the scattering length densities of lysozyme and buffer were matched and therefore lysozyme did not contribute to the scattering signal was determined as 46% D₂O, which agreed well with the reported value in the literature for lysozyme.²⁹ The ratio for HGH was determined as 48% D₂O. These ratios were used for all subsequent contrast-matched samples to mask the lysozyme or HGH and probe only the PEG portion of the PEG-protein conjugates. Lysozyme, HGH, and mPEG-PA were measured in 100% D₂O at dilute concentrations. Hydrogenated and deuterated monoPEG-lysozyme samples were measured in 100% D₂O and 46% D₂O, respectively. Deuterated monoPEG-HGH was measured in 48% D₂O. All samples that were originally lyophilized in pH 7.4 10 mM HEPES were resuspended into a volume of the appropriate water solvent to recover a pH 7.4 10 mM HEPES solution.

RESULTS AND DISCUSSION

SANS data are analyzed first in terms of a pair-distance distribution function (PDDF), which has the advantage of being model-independent, followed by the Guinier analysis that yields a more quantitative description of the distribution of mass in the scattering particle, followed by data fits to form factor models that discriminate between candidate structures.

PDDF. A first order classification of the shape of a scattering particle is obtained directly from $P(r)$, the PDDF.³⁰ $P(r)$ is related to the frequency of interatomic vector lengths, r , within the particle.³¹ $P(r)$ functions were calculated for all samples from the entire scattering curve [$I(q)$, to be shown below] using model-free inverse Fourier transformation.³⁰ Figure 1 displays the $P(r)$ analysis for lysozyme, unconjugated *hm*PEG-PA (hydrogenated mPEG propionaldehyde), and mono-*hm*PEG-lysozyme in 100% D₂O. The distance at which $P(r)$ falls to zero indicates the largest distance spanned by the scattering particle. This maximum dimension for mono-*hm*PEG-lysozyme, 21.20 ± 0.08 nm, is larger than the sum of the maximum dimension of lysozyme, 3.44 ± 0.06 nm, plus that of unconjugated *hm*PEG-PA, 13.33 ± 0.06 nm, where the latter dimensions are taken from the corresponding $P(r)$ functions. The statistical error bars correspond to 95% confidence limits.

Guinier Analysis. The Guinier approximation provides the radius of gyration, R_G , of the scattering particle. For low values of the scattering vector q , R_G can be extracted from the slope of $\ln I$ versus q^2 , as $\ln I(q) = \ln I(0) - [(R_G^2)/3]q^2$ provided the approximation is applied in the limit of $qR_G \ll 1$. The scattering vector q is defined as $(4\pi/\lambda) \sin(\theta)$ where λ is the wavelength of the incident neutrons and 2θ denotes the scattering angle.^{32,33} Values for R_G thus determined are listed in Table 1. Values for R_G for lysozyme and *hm*PEG-PA in 100% D₂O are comparable to those reported previously.^{9,34} As was the case with $P(r)$, R_G for mono-*hm*PEG-lysozyme,

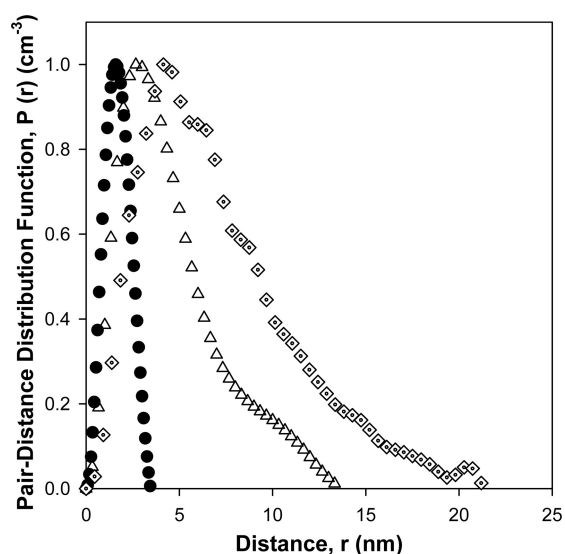


Figure 1. PDDFs, $P(r)$, for lysozyme (closed circles), hydrogenated mPEG-PA (open triangles), and hydrogenated monoPEG-lysozyme (dotted diamonds) in 100% D_2O containing 10 mM HEPES. The $P(r)$ maximum for each species is scaled to unity. The maximum extension of each particle is the point at which the function crosses the abscissa. The maximum extension of lysozyme, 3.44 ± 0.02 nm, plus the maximum extension of mPEG-PA, 13.33 ± 0.06 nm, is comparable to the maximum extension of monoPEG-lysozyme, 21.20 ± 0.08 nm. The statistical error bounding values correspond to 95% confidence limits.

6.8 ± 0.5 nm, is larger than the sum of R_G for lysozyme, 1.4 ± 0.2 nm, plus R_G for hmPEG-PA, 3.4 ± 0.3 nm. The statistical error bounding values correspond to 95% confidence limits.

Data Reduction and Form Factor Analysis. Using macros developed at NIST, all data were reduced and analyzed as $I(q)$ versus q using IGOR Pro software (WaveMetrics, Inc.).²⁸ Figures 2 and 3 permit comparison of the experimental scattering intensity profiles of lysozyme in 100% D_2O , containing 10 mM HEPES, and perdeuterated homopolymer mPEG-PA (dmPEG-PA) in 46% D_2O , containing 10 mM HEPES, with the theoretical smeared model curves for monodisperse spheres

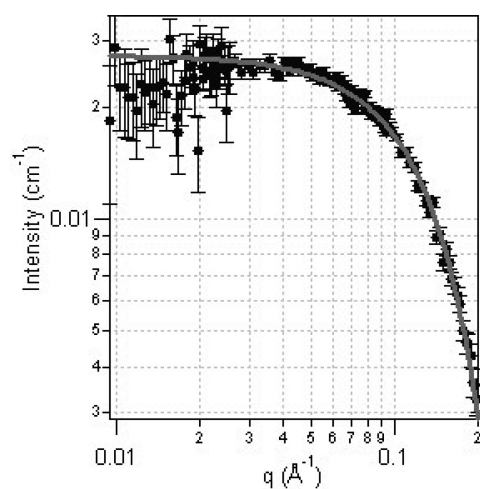


Figure 2. Comparison of the experimental scattering curve of lysozyme in 100% D_2O (filled circles), containing 10 mM HEPES, with the theoretical smeared curve of the sphere model for a monodisperse spherical particle with uniform scattering length density (solid line). Error bars represent the standard deviation of the intensity at each q value. For the fit, the scattering length density of the sphere was fixed at $2.56 \times 10^{-6} \text{ \AA}^{-2}$, and the scattering length density of the solvent was fixed at $6.33 \times 10^{-6} \text{ \AA}^{-2}$. The best fit generated a radius of 1.549 ± 0.001 nm. The statistical error bounding values correspond to 95% confidence limits.

(sphere model³³) and linear random coil polymer chains (Debye model³²), respectively. A dmPEG-PA sample was used to increase the signal-to-noise ratio when employing the contrast variation technique to measure the scattering profile of deuterated monoPEG-lysozyme (mono-dmPEG-lysozyme) in 46% D_2O , containing 10 mM HEPES. This is the ratio of D_2O necessary to contrast match the lysozyme, determined experimentally, allowing only the PEG portion of the conjugate to be probed. Lysozyme was well described by the sphere model with radius $R = 1.549 \pm 0.001$ nm (Figure 2), and the unconjugated dmPEG-PA was well described by the random coil Debye model with $R_G = 3.718 \pm 0.003$ nm (Figure 3). The statistical error bounding values correspond to 95% confidence limits. The

Table 1. Dimensions Generated for All Species for All Data Analysis Methods^a

species ^b	solvent with 10 mM HEPES (% D_2O)	data analysis method			
		DLS R_H (nm) ^{cd}	PDDF (nm) ^{ef}	Guinier R_G (nm) ^{gh}	model fitting (nm) ^{ij}
unmodified lysozyme	100	2.0 ± 0.9	max. ext. = 3.44 ± 0.02	1.4 ± 0.2	1.549 ± 0.001 (sphere, R_H)
hmPEG-PA	100	3.5 ± 1.4	max. ext. = 13.33 ± 0.06	3.4 ± 0.3	3.591 ± 0.001 (Debye, R_G)
mono-hmPEG-lysozyme	100	5.8 ± 2.6	max. ext. = 21.20 ± 0.08	6.8 ± 0.5	N/A
dmPEG-PA	46	N/A	N/A	N/A	3.718 ± 0.003 (Debye, R_G)
mono-dmPEG-lysozyme ^k	46	N/A	N/A	N/A	5.135 ± 0.006 (Debye, R_G)
mono-dmPEG-lysozyme ^k	46; plus 15 mg/mL lysozyme ^l	N/A	N/A	N/A	3.239 ± 0.002 (Debye, R_G)
mono-dmPEG-HGH ^m	48	N/A	N/A	N/A	5.012 ± 0.008 (Debye, R_G)

^aDimensions from DLS are also shown. ^bAbbreviations: hmPEG-PA, hydrogenated methoxy-PEG-propionaldehyde; dmPEG-PA, deuterated methoxy-PEG-propionaldehyde; hmono-hmPEG-lysozyme, hydrogenated monoPEG-lysozyme; mono-dmPEG-lysozyme, deuterated monoPEG-lysozyme; mono-dmPEG-HGH, deuterated monoPEG-HGH. ^c R_H is the hydrodynamic radius of an equivalent sphere determined by DLS, based on the intensity-weighted average distribution. ^dError values correspond to the half width at half max of the light scattering peak. ^eThe distance at which the PDDF falls to zero is an indication of the largest distance spanning the scattering particle, that is, the maximum extension (max. ext.) of the particle.^{30,31} ^fThe statistical error bounding values correspond to 95% confidence limits. ^gAccording to the Guinier approximation, the intensity at small q depends on the radius of gyration R_G of the scattering particle. ^hError values correspond to 95% confidence limits. ⁱExperimental scattering profiles were compared to theoretical smeared curves for monodisperse spheres (sphere model) and linear polymer chains (Debye model). ^jThe statistical error bounding values correspond to 95% confidence limits. ^kLysozyme portion of conjugate is contrast-matched for SANS. ^lConditions necessary to achieve an oncotic pressure similar to that of typical mammalian blood plasma. ^mHGH portion of conjugate is contrast-matched for SANS.

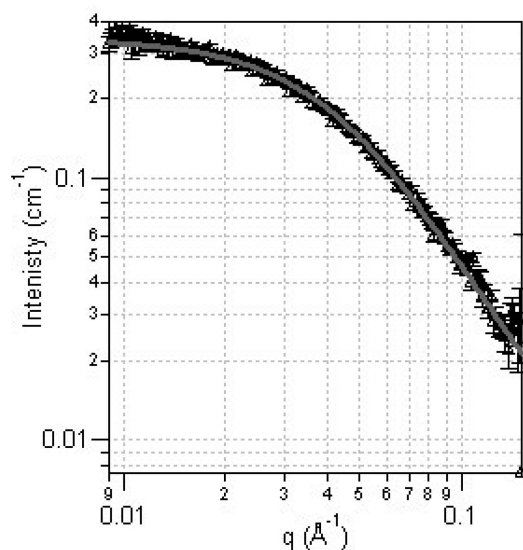


Figure 3. Comparison of the experimental scattering curve of deuterated mPEG-PA in 46% D₂O (open triangles), containing 10 mM HEPES, with the theoretical smeared curve of the Debye model for a random coil (solid line). Error bars represent the standard deviation of the intensity at each q value. The best fit generated a radius of gyration, R_G , of 3.718 ± 0.003 nm. The statistical error bounding values correspond to 95% confidence limits.

fitted radius of gyration for dm PEG-PA is somewhat smaller than the 6.7 nm z -average root-mean-square radius of gyration predicted by a light scattering correlation for PEG at 25 °C where $\langle R_G^2 \rangle = 4.08 \times 10^{-18} M_w^{1.16} \text{ cm}^2$.

To first test the suitability of the dumbbell model, the experimental scattering profile $I(q)$ of mono- dm PEG-lysozyme in 46% D₂O was compared to the theoretical smeared curve for a linear random coil polymer chain (Debye model). The quality of the random coil fit of the contrast-matched data in Figure 4 indicates that the conjugated PEG chain behaves as a random coil adjacent to the protein, supporting the dumbbell model.

As a counter-argument, the experimental scattering profile of mono- dm PEG-lysozyme in 46% D₂O, containing 10 mM HEPES, was then also compared to the theoretical smeared core-shell model for a spherical core of uniform scattering length density, surrounded by a shell having a different scattering length density; a successful fit to such a model would be consistent with the shroud model. The core-shell fit was applied in two different manners to attempt to achieve a satisfactory fit. In both cases, the scattering length densities of the core and solvent were set to be equal since the protein core was contrast-matched. In case 1, no other fitting constraints were applied, and the model fit generated a core radius of 2.98 ± 0.15 nm, a shell thickness of 0.08 ± 0.3 nm, and a shell scattering length density of $\rho_{\text{shell}} = 1.59 \times 10^{-6} \text{ \AA}^{-2}$; this scattering length density falls outside the range of the solvent ($\rho_{\text{solvent}} = 2.56 \times 10^{-6} \text{ \AA}^{-2}$) and pure d PEG ($\rho_{d\text{PEG}} = 5.73 \times 10^{-6} \text{ \AA}^{-2}$) and is therefore nonphysical for a mixture of d PEG and solvent. In case 2, the core radius was set to 1.55 nm, as previously determined by applying the sphere model to lysozyme SANS. The model then generated a shell thickness of 2.236 ± 0.002 nm, and the fitted scattering length density of the shell, $\rho_{\text{shell}} = 2.32 \times 10^{-6} \text{ \AA}^{-2}$, was again nonphysical. The fringes predicted by the fit to the smeared core-shell model

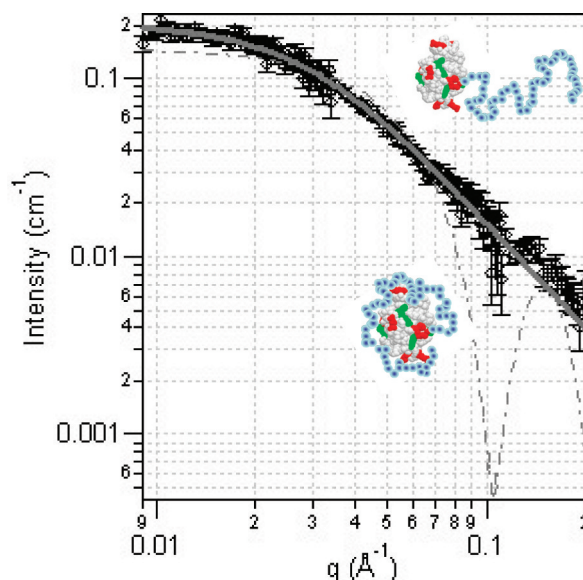


Figure 4. Comparison of the experimental scattering curve for deuterated monoPEG-lysozyme in 46% D₂O (dotted diamonds), containing 10 mM HEPES, with the theoretical smeared curve of the Debye model for a random coil (solid line) and the theoretical smeared core-shell model for a spherical particle of uniform scattering length density, surrounded by a shell having a different scattering length density (dashed line). Error bars represent the standard deviation of the intensity at each q value. The best fit generated a radius of gyration, R_G , of 5.135 ± 0.006 nm. The statistical error bounding values correspond to 95% confidence limits. Schematics qualitatively illustrate the dumbbell configuration (upper right) if the PEG chain followed the Debye model and the shroud configuration (lower left) if the PEG chain followed the core-shell model. Because of the contrast matching conditions, the protein is “invisible” to the neutrons in these measurements.

were absent in the experimental data. The statistical error bars correspond to 95% confidence limits.

On the basis of the agreement of contrast-matched SANS data for mono- dm PEG-LYZ with the random coil (Debye) model and not the core-shell model, we conclude that the conjugate adopts a dumbbell configuration (Figure 4) with the PEG chain forming an independent random coil domain rather than a shroud “wrapped” around the protein. As seen in Table 1, R_G for the lysozyme-conjugated dm PEG-PA chain is approximately 30% larger than that measured for free dm PEG-PA in 100% D₂O, containing 10 mM HEPES. This is expected because this PEG is end-anchored to the protein surface. As an isolated, nonadsorbing but end-grafted chain, configurational entropy dictates that it would be elongated relative to the unconjugated chain.³⁵

Extension to Additional Proteins. The measurements described in the previous section were extended to include a protein of pharmaceutical interest, HGH, covalently conjugated to a single ~ 20 kDa dm PEG-PA chain. The contrast variation technique was again employed to measure the scattering profile of mono- dm PEG-HGH in 48% D₂O, containing 10 mM HEPES, the experimentally determined D₂O content to contrast match HGH in buffer. The excellent agreement of the experimental scattering profile of mono- d PEG-HGH with the Debye model (Figure S2 in the Supporting Information, S3) again is consistent with the grafted PEG chain existing as a random coil adjacent to the protein, that is, adopting the dumbbell configuration.

Determining the Configuration of the PEG Chain in Plasmalike Environments. All measurements described thus far were in dilute solution, but blood has a large oncotic pressure that may influence the PEG conformation in a PEGylated therapeutic protein. To determine the behavior of the conjugated PEG chain as it might exist in blood, we mimicked the oncotic pressure of plasma by dissolving the mono-*dm*PEG–lysozyme (20 kDa *dm*PEG–PA) in a 15 mg/mL solution of unconjugated lysozyme, the concentration of lysozyme necessary to create an oncotic pressure typical of mammalian plasma, ~ 2500 Pa, in 46% D₂O, containing 10 mM HEPES, to contrast-match lysozyme. The data are again well described by the random coil model, consistent with the dumbbell configuration, but now, R_G for the PEG conjugate, 3.238 ± 0.002 nm, is about 15% smaller than that for an unconjugated *dm*PEG–PA chain in 46% D₂O, containing 10 mM HEPES, 3.718 ± 0.003 nm (Figure S3 in the Supporting Information, S4). The statistical error bounding values correspond to 95% confidence limits. Evidently, competition for water in the plasmalike environment causes a small decrease of the excluded volume of the conjugated PEG chain but does not alter the tendency to adopt a random coil configuration. This is consistent with the effect of high conjugate concentration noted by He et al.²³

Implications. It is well established that the covalent attachment of PEG increases in vivo blood circulation times for protein therapeutics. The implications of the dumbbell configuration for the steric protection of a conjugated protein can now be considered. In the case of a single grafted PEG chain per protein, the dumbbell configuration leaves part of the protein unprotected, but it does provide a locally strong steric repulsion force to protect the conjugated part of the molecule. In contrast, the shroud configuration, if it occurred, would have spread its protective effect over a larger fraction of the protein surface. Yet, by spreading a limited polymer mass over a large area, the local segmental density in any one region would be rather low and would afford only a weak and short-range steric repulsion, since the range of steric forces imparted by grafted polymer chains is dictated by the normal extension of the chain away from the surface and the magnitude scales with the local segment density. The random coil dumbbell configuration offers strong but more highly localized protection of the protein. For example, the nearer the site of PEGylation is to a binding epitope, the more effective its protection would be. Similar considerations come into play concerning the degree to which a conjugated PEG chain could disrupt access to a protein active site.

CONCLUSION

SANS was employed with a contrast variation technique to probe only the PEG portion of the PEG–protein conjugate to directly determine the configuration of a single ~ 20 kDa PEG chain covalently attached to lysozyme or HGH. Analyses of the scattering data in terms of the pairwise distance distribution function, the Guinier analysis of conjugate radius of gyration, and model fitting to the Debye random coil polymer scattering form factor are consistent with a dumbbell model in which the PEG chain behaves as a random coil adjacent to the protein and directly challenge the more commonly presumed shroud configuration in which the PEG chain wraps around the protein, creating a shielding effect.

ASSOCIATED CONTENT

Supporting Information

Characterization of the PEGylated conjugates and synthesis of the perdeuterated methoxy-PEG–propionaldehyde, SANS

data, and model fits for lysozyme in the plasmalike environment and for HGH. This material is available free of charge via the Internet at <http://pubs.acs.org>.

AUTHOR INFORMATION

Corresponding Author

*Tel: 412-268-3857. E-mail: todd@andrew.cmu.edu (T.M.P.).
Tel: 412-268-1159. E-mail: tilton@andrew.cmu.edu (R.D.T.).

ACKNOWLEDGMENTS

The identification of commercial products does not imply endorsement by the National Institute of Standards and Technology nor does it imply that these are the best for the purpose. This material is based on work supported by the National Science Foundation under Grant CBET 0755284 and utilized facilities supported in part by the National Science Foundation under Agreement No. DMR-0454672. We thank Dr. Reddy's Laboratories, LLC, and Genentech, Inc., for their generous donation of mPEG–propionaldehyde and HGH, respectively. A portion of this research was conducted at the Center for Nanophase Materials Sciences (CNMS), which is sponsored at Oak Ridge National Laboratory (ORNL) by the Office of Basic Energy Sciences, U.S. Department of Energy, through the CNMS user program (user proposal number: CNMS2009-212). A portion of this research at ORNL's High Flux Isotope Reactor was sponsored by the Scientific User Facilities Division, Office of Basic Energy Sciences, U.S. Department of Energy. This work benefited from DANSE software developed under NSF award DMR-0520547.

REFERENCES

- (1) Pai, S. S., Przybycien, T. M., and Tilton, R. D. (2009) Poly(ethylene glycol)-Modified Proteins: Implications for Poly(lactide-co-glycolide)-Based Microsphere Delivery. *AAPS J.* 11, 88–98.
- (2) Freitas, D. d. S., and Abrahao-Neto, J. (2010) Biochemical and biophysical characterization of lysozyme modified by PEGylation. *Int. J. Pharm.* 392, 111–117.
- (3) Michaelis, M., Cinatl, J., Cinatl, J., Pouckova, P., Langer, K., Kreuter, J., and Matousek, J. (2002) Coupling of the antitumoral enzyme bovine seminal ribonuclease to polyethylene glycol chains increases its systemic efficacy in mice. *Anti-Cancer Drugs* 13, 149–154.
- (4) Harris, J. M., Martin, N. E., and Modi, M. (2001) Pegylation—A novel process for modifying pharmacokinetics. *Clin. Pharmacokinet.* 40, 539–551.
- (5) Greenwald, R. B., Choe, Y. H., McGuire, J., and Conover, C. D. (2003) Effective drug delivery by PEGylated drug conjugates. *Adv. Drug Delivery Rev.* 55, 217–250.
- (6) Shu, J. Y., Tan, C., DeGrado, E. D., and Xu, T. (2008) New design of helix bundle peptide-polymer conjugates. *Biomacromolecules* 9, 2111–2117.
- (7) Morar, S., Schrimsher, J. L., and Chavez, M. D. (2006) PEGylation of Proteins: A Structural Approach: Structural properties of PEGylated proteins could play an increasingly important role in developing optimal therapeutic protein drugs. *Biopharm. Int.* 19, 34–44.
- (8) Daly, S. M., Przybycien, T. M., and Tilton, R. D. (2005) Adsorption of Poly(ethylene glycol)-Modified Ribonuclease A to a Poly(lactide-co-glycolide) Surface. *Biotechnol. Bioeng.* 90, 856–868.
- (9) Daly, S. M., Przybycien, T. M., and Tilton, R. D. (2005) Adsorption of Poly(ethylene glycol)-Modified Lysozyme to Silica. *Langmuir* 21, 1328–1337.
- (10) Diwan, M., and Park, T. G. (2003) Stabilization of recombinant interferon- α by pegylation for encapsulation in PLGA microspheres. *Int. J. Pharm.* 252, 111–122.
- (11) Diwan, M., and Park, T. G. (2001) Pegylation enhances protein stability during encapsulation in PLGA microspheres. *J. Controlled Release* 73, 233–244.

- (12) Molek, J. R., and Zydney, A. L. (2006) Ultrafiltration Characteristics of Pegylated Proteins. *Biotechnol. Bioeng.* 95, 474–482.
- (13) Fee, C. J., and Alstine, J. M. V. (2004) Prediction of the Viscosity Radius and the Size Exclusion Chromatography Behavior of PEGylated Proteins. *Bioconjugate Chem.* 15, 1304–1313.
- (14) Manjula, B. N., Tsai, A., Upadhyaya, R., Perumalsamy, K., Smith, P. K., Malavalli, A., Vandegriff, K., Winslow, R. M., Intaglietta, M., Prabhakaran, M., Friedman, J. M., and Acharya, A. S. (2003) Site-Specific PEGylation of Hemoglobin at Cys-93(β): Correlation between the Colligative Properties of the PEGylated Protein and the Length of the Conjugated PEG Chain. *Bioconjugate Chem.* 14, 464–472.
- (15) Garcia-Arellano, H., Valderrama, B., Saab-Rincon, G., and Vazquez-Duhalt, R. (2002) High Temperature Biocatalysis by Chemically Modified Cytochrome c. *Bioconjugate Chem.* 13, 1336–1344.
- (16) Kozlowski, A., Charles, S. A., and Harris, J. M. (2001) Development of Pegylated Interferons for the Treatment of Chronic Hepatitis C. *BioDrugs* 15, 419–429.
- (17) Roberts, M. J., Bentley, M. D., and Harris, J. M. (2002) Chemistry for peptide and protein PEGylation. *Adv. Drug Delivery Rev.* 54, 459–476.
- (18) Schmidt, P. G., Campbell, K. M., Hinds, K. D., and Cook, G. P. (2007) PEGylated bioactive molecules in biodegradable polymer microparticles. *Expert Opin. Biol. Ther.* 7, 1427–1436.
- (19) Harris, J. M., and Chess, R. B. (2003) Effect of PEGylation on pharmaceuticals. *Nature Rev. Drug Discovery* 2, 214–221.
- (20) Abuchowski, A., Es, T. V., Palczuk, N. C., and Davis, F. F. (1977) Alteration of Immunological Properties of Bovine Serum Albumin by Covalent Attachment of Polyethylene Glycol. *J. Biol. Chem.* 252, 3578–3581.
- (21) Li, D., Manjula, B. N., and Acharya, A. S. (2006) Extension Arm Facilitated PEGylation of Hemoglobin: Correlation of the Properties with the Extent of PEGylation. *Protein J.* 25, 263–274.
- (22) Fee, C. J. (2007) Size comparison between proteins PEGylated with branched and linear poly(ethylene glycol) molecules. *Biotechnol. Bioeng.* 98, 725–731.
- (23) He, L., Wang, H., Garamus, V. M., Hanley, T., Lensch, M., Gabius, H.-J., Fee, C. J., and Middelberg, A. (2010) Analysis of MonoPEGylated Human Galectin-2 by Small-Angle X-ray and Neutron Scattering: Concentration Dependence of PEG Conformation in the Conjugate. *Biomacromolecules* 11, 3504–3510.
- (24) Svergun, D. I., Ekström, F., Vandegriff, K. D., Malavalli, A., Baker, D. A., Nilsson, C., and Winslow, R. M. (2008) Solution Structure of Poly(ethylene) Glycol-Conjugated Hemoglobin Revealed by Small-Angle X-Ray Scattering: Implications for a New Oxygen Therapeutic. *Biophys. J.* 94, 173–181.
- (25) Kinstler, O. B., Gabriel, N. E., Farrar, C. E., and DePrince, R. B. (1998) N-Terminally chemically modified protein compositions and methods. U.S. Patent.
- (26) Sreerama, N., and Woody, R. W. (2000) Estimation of protein secondary structure from CD spectra: Comparison of CONTIN, SELCON and CDSSTR methods with an expanded reference set. *Anal. Biochem.* 287, 252–260.
- (27) Glinka, C. J., Barker, J. G., Hammouda, B., Krueger, S., Moyer, J. J., and Orts, W. J. (1998) The 30 m Small-Angle Neutron Scattering Instruments at the National Institute of Standards and Technology. *J. Appl. Crystallogr.* 31, 430–445.
- (28) Kline, S. R. (2006) Reduction and analysis of SANS and USANS data using IGOR Pro. *J. Appl. Crystallogr.* 39, 895–900.
- (29) Stuhmann, H. B., and Fuess, H. (1976) A Neutron Small-Angle Scattering Study of Hen Egg-White Lysozyme. *Acta Crystallogr., Sect. A, Cryst. Phys., Diffr., Theor. Gen. Crystallogr.* A32, 67–74.
- (30) Glatter, O., and Kratky, O., Eds. (1982) *Small Angle X-ray Scattering*, Vol. 515, Academic Press Inc., New York, NY.
- (31) Hong, X., and Hao, Q. (2009) High resolution pair-distance distribution function $P(r)$ or protein solutions. *Appl. Phys. Lett.* 94, 1–3.
- (32) Svergun, D. I., and Koch, M. H. J. (2003) Small-angle scattering studies of biological macromolecules in solution. *Rep. Prog. Phys.* 66, 1735–1782.
- (33) Roe, R.-J. (2000) *Methods of X-Ray and Neutron Scattering in Polymer Science*, pp 1–331, Oxford University Press, Inc., New York.
- (34) Pai, S. S., Przybycien, T. M., and Tilton, R. D. (2010) Protein PEGylation Attenuates Adsorption and Aggregation on a Negatively Charged and Moderately Hydrophobic Polymer Surface. *Langmuir* 26, 18231–18238.
- (35) Fleer, G. J., Stuart, M. A. C., Scheutjens, J. M. H. M., Cosgrove, T., and Vincent, B. (1993) *Polymers at Interfaces*, pp 1–502, Chapman & Hall, London.